Secure Systems Design and Technology Development. Veliko Tarnovo, Bulgaria
Proceedings of the International Scientific Conference, 2026. Volume I, 387-398

Competing Thermodynamic and Radiative Effects on Atmospheric Circulation in Polluted Environments

Mihai Petrov
dept. of Natural Sciencies
Burgas State University "Pr. Dr. Assen Zlatarov"
Burgas, Bulgaria
mihai-petrov@uniburgas.bg;
ORCID: 0000-0003-0811-1250

***Abstract*—This study develops a unified method linking thermodynamic processes and radiative feedbacks in a human altered atmosphere, combining an adiabatic calorimetric perspective with a radiation balance model to describe wind changes. Air pollutants produce two competing effects: thermodynamic damping, where polyatomic gases and aerosols modify air properties and reduce wind speed, and radiative effects linked to increased reflectivity that can enhance or stabilize winds. A feedback ratio determines which mechanism dominates. When thermodynamic damping prevails, wind stilling occurs in regions with high absorbing aerosols; when radiative effects dominate, winds remain stable or slightly intensify in scattering aerosol environments. The regime depends strongly on aerosol composition, with scattering particles promoting stability and absorbing particles driving destabilization. These results show that accurate climate projections require considering aerosol composition alongside greenhouse gases, highlighting complex non linear coupling between air quality and atmospheric circulation.**

Keywords*— *adiabatical constant, damping, pollutants, speed of wind.

I. Introduction

Human activity alters the atmosphere through greenhouse gases and aerosols, affecting temperature, pressure, specific heat capacity (c_p), and the adiabatic constant (γ), which control climate dynamics. Radiatively active gases, especially CO_2 and CH_4, drive warming, with CO_2 contributing about 75% of emissions [1], [2], [3], [4], [5], [6]. Fossil fuel use also reduces O_2 and increases polyatomic gases and aerosols [7], [8]. These changes modify thermodynamic properties: aerosols affect radiation and heat transfer [9], [10], while cp decreases (~1010→992 $J \cdot kg^{-1} \cdot K^{-1}$) and γ (~1.101→1.061) [11], [12], [10], [13], potentially reducing wind speed by up to 20% [14]. Aerosols also alter radiative balance by enhancing cloud reflectivity (Twomey effect) [15], [16], while land use and black carbon modify albedo [17], [18], [19]. Marine aerosols increase reflectivity, whereas black carbon reduces it and affects circulation [20], [21], [22].

II. Materials and Methods

A quantitative description of atmospheric conditions affected by greenhouse pollutants, including the relationship between air temperature and variations in pollutant concentration, was reported in [1].

$$\Delta T = (\gamma - 1) \cdot \frac{\Delta C \cdot T}{C} \tag{1}$$

here, C denotes the overall molar concentration of atmospheric air, while ΔC corresponds to the variation in concentration produced by the presence of greenhouse pollutants, and T represents the atmospheric temperature. Estimated molar concentrations allow evaluation of ΔT from ΔC. Over the past 50 years, global mean temperature has risen approximately linearly [3], mainly driven by CO_2, which accounts for ~75% of fossil fuel emissions [6], [7]. Since the industrial era, emissions have increased by about 70% (1970–2004) [5]. This warming can be described using thermodynamic and calorimetric approaches [6]. CO_2 growth is also linked to a net O_2 decline due to incomplete photosynthetic compensation [7]. The present study applies a combined adiabatic calorimetric formulation following [6].

$$\Delta T(t) = \frac{\Delta Q(t) + c.(\Delta m(O_2) - \Delta m(CO_2)).(T - T_{eff})}{c.[m - \Delta m(O_2) + \Delta m(CO_2)]} \tag{2}$$

The atmospheric mass is m ≈ 5.13 × 10^{18} kg [23], with effective temperature T_{eff} =253 K and specific heat capacity c ≈ 1007 $J \cdot kg^{-1} \cdot K^{-1}$ [6], [23]. About 60% of excess heat ΔQ is absorbed by the Oceans [24], [25], [26],

Online ISSN 3044-7771
https://doi.org/10.68302/std2026.vol1.97

which also take up ~30% of atmospheric CO_2 [27], [28], [29], [30], [31]. Accordingly, atmospheric heat and mass terms are writtten as follows:

$$\Delta m(CO_2) \to 0.7 \cdot \Delta m(CO_2)\ \Delta Q(t) \to 0.4 \cdot \Delta Q(t) \tag{3}$$

Therefore (2) incorporating the absorption of both heat and carbon dioxide by the Oceans, can be expressed as:

$$\Delta T(t) = \frac{0.4 \cdot \Delta Q(t) + c.\left(\Delta m(O_2) - 0.7 \cdot \Delta m(CO_2)\right).(T - T_{eff})}{c.[m - \Delta m(O_2) + 0.7 \cdot \Delta m(CO_2)]} \tag{4}$$

Since ~60% of heat is absorbed by the Oceans, only ~40% remains in the atmosphere; thus the annual retained heat is 0.4 × 3.05×10^{20} J/year = 1.22×10^{20} J/year. Temperature variations calculated from (4) are shown in the last column of Table 1.

TABLE 1 CALCULATIONS OF THE VARIATION OF ATMOSPHERE'S TEMPERATURE WITH TIME [6]

No	Year	ΔT_r; (°C)	ΔQ;(J)	Δm (CO_2); (kg)	Δm (O_2); (kg)	ΔT ;(°C)
0	1980	0	0	0	0	0
1	1981	0.03	$1.22\cdot10^{20}$	$1.08\cdot10^{13}$	$1.8\cdot10^{13}$	0.023
2	1982	0.05	$2.44\cdot10^{20}$	$1.62\cdot10^{13}$	$1.9\cdot10^{13}$	0.047
3	1983	0.07	$3.66\cdot10^{20}$	$2.7\cdot10^{13}$	$2\cdot10^{13}$	0.070
4	1984	0.09	$4.88\cdot10^{20}$	$3.78\cdot10^{13}$	$2.2\cdot10^{13}$	0.094
5	1985	0.11	$6.1\cdot10^{20}$	$4.86\cdot10^{13}$	$2.3\cdot10^{13}$	0.117
6	1986	0.13	$7.32\cdot10^{20}$	$5.4\cdot10^{13}$	$2.31\cdot10^{13}$	0.141
7	1987	0.15	$8.54\cdot10^{20}$	$5.94\cdot10^{13}$	$2.4\cdot10^{13}$	0.165
8	1988	0.18	$9.76\cdot10^{20}$	$6.48\cdot10^{13}$	$2.42\cdot10^{13}$	0.188
9	1989	0.19	$1.1\cdot10^{21}$	$6.75\cdot10^{13}$	$2.5\cdot10^{13}$	0.212
10	1990	0.22	$1.22\cdot10^{21}$	$7.02\cdot10^{13}$	$2.53\cdot10^{13}$	0.235
11	1991	0.26	$1.34\cdot10^{21}$	$7.56\cdot10^{13}$	$2.56\cdot10^{13}$	0.259
12	1992	0.32	$1.46\cdot10^{21}$	$8.1\cdot10^{13}$	$2.6\cdot10^{13}$	0.283
13	1993	0.34	$1.59\cdot10^{21}$	$9.18\cdot10^{13}$	$2.62\cdot10^{13}$	0.306
14	1994	0.36	$1.71\cdot10^{21}$	$1.03\cdot10^{14}$	$2.71\cdot10^{13}$	0.330
15	1995	0.37	$1.83\cdot10^{21}$	$1.13\cdot10^{14}$	$2.74\cdot10^{13}$	0.353
16	1996	0.39	$1.95\cdot10^{21}$	$1.19\cdot10^{14}$	$2.78\cdot10^{13}$	0.377
17	1997	0.41	$2.07\cdot10^{21}$	$1.24\cdot10^{14}$	$2.8\cdot10^{13}$	0.400
18	1998	0.42	$2.2\cdot10^{21}$	$1.3\cdot10^{14}$	$2.9\cdot10^{13}$	0.424
19	1999	0.43	$2.32\cdot10^{21}$	$1.35\cdot10^{14}$	$3\cdot10^{13}$	0.448
20	2000	0.45	$2.44\cdot10^{21}$	$1.46\cdot10^{14}$	$3.1\cdot10^{13}$	0.471
21	2001	0.46	$2.56\cdot10^{21}$	$1.67\cdot10^{14}$	$3.12\cdot10^{13}$	0.495
22	2002	0.47	$2.68\cdot10^{21}$	$1.89\cdot10^{14}$	$3.2\cdot10^{13}$	0.518
23	2003	0.5	$2.81\cdot10^{21}$	$2\cdot10^{14}$	$3.3\cdot10^{13}$	0.542
24	2004	0.54	$2.93\cdot10^{21}$	$2.05\cdot10^{14}$	$3.4\cdot10^{13}$	0.565
25	2005	0.58	$3.05\cdot10^{21}$	$2.16\cdot10^{14}$	$3.43\cdot10^{13}$	0.589
26	2006	0.59	$3.17\cdot10^{21}$	$2.22\cdot10^{14}$	$3.5\cdot10^{13}$	0.612
27	2007	0.6	$3.29\cdot10^{21}$	$2.27\cdot10^{14}$	$3.55\cdot10^{13}$	0.636
28	2008	0.61	$3.42\cdot10^{21}$	$2.32\cdot10^{14}$	$3.6\cdot10^{13}$	0.659
29	2009	0.62	$3.54\cdot10^{21}$	$2.38\cdot10^{14}$	$3.7\cdot10^{13}$	0.683
30	2010	0.63	$3.66\cdot10^{21}$	$2.43\cdot10^{14}$	$3.8\cdot10^{13}$	0.707
31	2011	0.65	$3.78\cdot10^{21}$	$2.54\cdot10^{14}$	$3.81\cdot10^{13}$	0.730
32	2012	0.68	$3.9\cdot10^{21}$	$2.97\cdot10^{14}$	$3.9\cdot10^{13}$	0.754
33	2013	0.7	$4.03\cdot10^{21}$	$3.24\cdot10^{14}$	$3.94\cdot10^{13}$	0.777
34	2014	0.74	$4.15.10^{21}$	$3.4\cdot10^{14}$	$3.9\cdot10^{13}$	0.800
35	2015	0.78	$4.27\cdot10^{21}$	$3.46\cdot10^{14}$	$3.98\cdot10^{13}$	0.824
36	2016	0.8	$4.39\cdot10^{21}$	$3.67\cdot10^{14}$	$4\cdot10^{13}$	0.848
37	2017	0.81	$4.51\cdot10^{21}$	$3.89\cdot10^{14}$	$4.1\cdot10^{13}$	0.871
38	2018	0.82	$4.64\cdot10^{21}$	$4\cdot10^{14}$	$4.11\cdot10^{13}$	0.895
39	2019	0.83	$4.76\cdot10^{21}$	$4.05\cdot10^{14}$	$4.2\cdot10^{13}$	0.918
4 0	2020	0.85	$4.88\cdot10^{21}$	$4.16\cdot10^{14}$	$4.22\cdot10^{13}$	0.942

The accumulation of anthropogenic heat in the atmosphere, ΔQ, can be expressed in terms of the corresponding variation in atmospheric temperature, ΔT, as indicated by empirical observations, as follows:

$$\Delta Q_{emp} = c \cdot m_{atm} \cdot \Delta T_r \tag{5}$$

where m_{atm} is the mass of atmosphere; ΔT_r are the real registered values of the variations of the temperature; c - specific heat capacity of atmopheric air. The combination of the adiabatic method, expressed by (1), and the thermodynamic method, described by (5), allows the formulation of a more general expression that incorporates additional parameters:

$$\Delta Q_{emp} = (\gamma - 1) \cdot c \cdot m_{atm} \cdot \frac{T}{C} \cdot \Delta C \tag{6}$$

here, T represents the current average global atmospheric temperature, C is the total molar concentration of the atmosphere, and ΔC denotes the concentration change caused by greenhouse gas accumulation. The specific heat capacity at constant pressure (c_p) is the energy needed to raise a unit mass of gas by one degree and is a mass weighted average in mixtures [11]. The atmosphere is mainly N_2 and O_2, with smaller amounts of Ar and greenhouse gases (CO_2, CH_4), whose molecular properties affect heat capacity [11], [32]. Increasing their concentration can reduce specific heat capacity at constant pressure - c_p [32], [33]. Lower c_p reduces warming energy and increases the dry adiabatic lapse rate dT/dz, affecting stability and convection [34], [35], [36].

$$\frac{dT}{dz} = -\frac{g}{c_p} \tag{7}$$

Here, dT/dz is the temperature gradient, z is altitude, g = 9.83 m/s², and c_p is the specific heat capacity. Rising air cools adiabatically [25], and higher lapse rates increase instability, convection, and extreme weather [36], [37]. Small gradient changes under high greenhouse gas levels can intensify storms, while γ variations are smaller than c_p effects [38], [39]. Albedo controls radiation balance [40], [41]. Scattering aerosols increase reflectivity, while black carbon reduces it and warms the atmosphere [42], [43]. Aerosols also enhance cloud brightness, affecting radiation, microclimate, and circulation [44], [45], [46], [47], [48], [49].

The application of (4) gives possibility to obtain an expession for the specific heat capacity that is written as follows:

$$c = \frac{\Delta Q}{\left(m - \Delta m(O_2) + \Delta m(CO_2)\right)\cdot \Delta T - \left(\Delta m(O_2) - \Delta m(CO_2)\right)\cdot (T - T_{eff})} = \frac{\Delta Q}{Z}$$

(8)

where Z is the expression of denominator from the left side of (8).

Atmospheric air mass dynamics are governed by a complex synergy of factors defined by numerous physicochemical parameters. A primary phenomenon associated with these displacements is wind, which represents the vector quantity of air motion. Wind velocity and flow patterns are subject to modulation by atmospheric constituents, including anthropogenic or natural aerosols and greenhouse gases, which alter the thermal and barometric gradients within the troposphere.

To characterize the vertical transport of air masses under varying thermodynamic conditions, the velocity of ascending air currents is evaluated using the following expression [50], [51]:

$$u = g \cdot h \cdot \sqrt{\frac{2}{c_p.T}} \tag{9}$$

where c_p is the specific heat capacity at constant pressure, T is the atmospheric air temperature, g is the gravitational acceleration, and h denotes altitude. This relationship shows that vertical wind speed depends on atmospheric height, temperature, and the molecular properties of the air mixture. The specific heat capacity at constant pressure (c_p) is given as follows [50], [52], [53]:

$$c_p = \frac{\gamma \cdot R}{\gamma - 1} \tag{10}$$

where R is the universal gas constant and γ is the adiabatic constant of the atmosphere. Substituting (10) into (9) yields the following result:

$$u = g \cdot h \cdot \sqrt{\frac{2}{C_p.T}} = gh \cdot \sqrt{\frac{2}{R}} \cdot \sqrt{\frac{\gamma - 1}{\gamma.T}} \tag{11}$$

The aim is to derive an expression for wind speed variation (Δu) as a function of changes in the adiabatic constant (Δγ), temperature (ΔT), and specific heat capacity (Δc_p). From (11) the following formal operation is obtained:

$$u^2 = \frac{g^2.h^2.\sqrt{4\cdot(\gamma-1)}}{\sqrt{\gamma \cdot c_p.R \cdot T^2}} = \frac{2 \cdot g^2.h^2.\sqrt{\gamma - 1}}{T \cdot \sqrt{\gamma \cdot R \cdot c_p}} \tag{12}$$

Differentiation of (12) makes it possible to obtain an expression that relates the variation of wind speed (Δu) to the proper value of speed u.

$$2.u.\Delta u = \frac{2.g^2.h^2}{\sqrt{R}} \cdot \left(\sqrt{\frac{\gamma - 1}{\gamma.c_p.T^2}}\right)' \tag{13}$$

The derivative of the term $\left(\sqrt{\frac{\gamma - 1}{\gamma.c_p.T^2}}\right)'$ can be examined under conditions where two consecutive parameters are held constant while the third varies ($\gamma = const$ or $T = const$ or $c_p = const$).

$$\left(\sqrt{\frac{\gamma - 1}{\gamma.c_p.T^2}}\right)'_{\gamma \neq const} = \frac{1}{2 \cdot \sqrt{c_p.T^2}} \cdot \sqrt{\frac{\gamma}{\gamma - 1}} \cdot \frac{\Delta\gamma}{\gamma^2}; \tag{14}$$

$$\left(\sqrt{\frac{\gamma - 1}{\gamma.c_p.T^2}}\right)'_{T \neq const} = -\sqrt{\frac{\gamma - 1}{\gamma \cdot c_p}} \cdot \frac{\Delta T}{T^2}; \tag{15}$$

$$\left(\sqrt{\frac{\gamma - 1}{\gamma.c_p.T^2}}\right)'_{c_p \neq const} = -\frac{1}{2} \cdot \sqrt{\frac{\gamma - 1}{\gamma \cdot}} \cdot \frac{\Delta c_p}{c_p \cdot \sqrt{c_p}}; \tag{16}$$

Taking into account (14), (15), and (16), then (13) can be written as follows:

$$u.\Delta u = \frac{g^2.h^2}{\sqrt{R}} \cdot \left(\frac{1}{2.T.\sqrt{c_p}} \cdot \sqrt{\frac{\gamma}{\gamma - 1}} \cdot \frac{\Delta\gamma}{\gamma^2} - \sqrt{\frac{\gamma - 1}{\gamma \cdot c_p}} \cdot \frac{\Delta T}{T^2} - \frac{1}{2} \cdot \sqrt{\frac{\gamma - 1}{\gamma \cdot T^2}} \cdot \frac{\Delta c_p}{c_p \cdot \sqrt{c_p}}\right) \tag{17}$$

Then, (11) can be written as follows:

$$g^2.h^2 = \frac{u^2 \cdot c_p \cdot T}{2} \tag{18}$$

Substituting (18) into (17) yields the following result:

$$\frac{\Delta u}{u} = \frac{c_p.T}{\sqrt{R}} \cdot \left(\frac{1}{2.T.\sqrt{c_p}} \cdot \sqrt{\frac{\gamma}{\gamma - 1}} \cdot \frac{\Delta\gamma}{\gamma^2} - \sqrt{\frac{\gamma - 1}{\gamma \cdot c_p}} \cdot \frac{\Delta T}{T^2} - \frac{1}{2} \cdot \sqrt{\frac{\gamma - 1}{\gamma \cdot T^2}} \cdot \frac{\Delta c_p}{c_p \cdot \sqrt{c_p}}\right) \tag{19}$$

$$\frac{\Delta u}{u} = \frac{c_p.T}{\sqrt{R}} \cdot \sqrt{\frac{\gamma}{(\gamma - 1)\cdot c_p}} \cdot \left(\frac{1}{2.T} \cdot \frac{\Delta\gamma}{\gamma^2} - \left(\frac{\gamma - 1}{\gamma}\right)\frac{\Delta T}{T^2} - \frac{\gamma - 1}{2 \cdot \gamma \cdot T} \cdot \frac{\Delta c_p}{c_p}\right) \tag{20}$$

Thus, the expression for the relative change in wind speed $\Delta u/u$ is a multivariable function that depends on the differentials of the adiabatic constant ($\Delta\gamma$), absolute temperature (ΔT), and specific heat capacity at constant pressure (ΔC_p). This formulation makes it possible to assess how localized perturbations in thermal properties and gas constants propagate as variations in wind kinetic behavior. By isolating the terms associated with $\Delta\gamma$, ΔT, and ΔCp, the model can identify the relative contribution of each thermodynamic parameter to the overall instability of the velocity field.

The albedo of biosphere components is influenced by temperature changes caused by the presence of pollutant aerosols in the atmosphere. It plays an important role in the formation of the local microclimate. An increase in global temperature leads to a corresponding increase in albedo [48]. The variation of albedo is written as follows [48]:

$$\Delta A = \frac{16 \cdot \varepsilon \cdot \sigma}{I_{sc}} \cdot T_{eff}^3 \cdot \left(\frac{1}{m.c} \cdot \left(\Delta Q - \frac{Q.\Delta m}{m} \right) - \Delta T \right) \quad (21)$$

Pollutants affect both heat trapping and air motion, while albedo further modifies the local microclimate. The value of ΔT, expressed as a function of albedo change (ΔA), can be substituted into (21), yielding the following expression for Δu/u:

$$\frac{\Delta u}{u} = \frac{\gamma}{(\gamma-1)\cdot\sqrt{R}} \cdot \left[\frac{\Delta\gamma}{2\cdot\gamma^2} - \frac{(\gamma-1)\cdot T}{\gamma} \cdot \frac{\Delta c_p}{2\cdot c_p} - \frac{(\gamma-1)}{\gamma\cdot T} \cdot \left(\frac{\Delta Q}{m\cdot c} - \frac{Q\cdot\Delta m}{m^2\cdot c} \right) + \frac{(\gamma-1)}{\gamma\cdot T} \cdot \frac{\Delta A}{K} \right] \quad (22)$$

where : $K = \frac{16 \cdot \varepsilon \cdot \sigma}{I_{sc}} \cdot T_{eff}^3$; $T_{eff} = T - \frac{Q}{m.c}$

The final expression shows that wind speed depends on both thermodynamic and radiative processes in the atmosphere. Changes in the adiabatic constant, specific heat capacity, and temperature would affect air stability and wind circulation. Higher pollutant concentrations could decrease the adiabatic constant and suppress normal adiabatic cooling, leading to weaker wind development. Pollutants such as PM2.5, PM10, black carbon, and greenhouse gases would contribute to this thermodynamic damping. In contrast, scattering aerosols increase albedo and could partly compensate for wind reduction by reflecting more solar radiation. Thus, wind behavior is controlled by the balance between thermodynamic damping and albedo-driven stabilization.

III. Results and Discussion

To evaluate the reliability of the obtained results through comparison with empirical atmospheric data, the proposed calorimetric approach was utilized to recalculate the atmospheric specific heat capacity. Using the formula defined in (8) for specific heat capacity values, the calculated results are presented in Table 2.

TABLE 2 THE DYNAMICS OF VARIATIONS IN ATMOSPHERIC OXYGEN AND CARBON DIOXIDE CONCENTRATIONS [6]

Year	ΔTr; °C	Δm(CO2) x10^{13}; (kg)	Δm(O2) x10^{13}; (kg)	m x10^{18}; (kg)	m x ΔTr; x10^{18}	Z x10^{18}	ΔQ x10^{20}; (J)
1981	0.03	1.08	1.8	5.49999	0.165	0.164752	1.22
1982	0.05	1.62	1.9	5.5000	0.275	0.274924	2.44
1983	0.07	2.7	2	5.50001	0.385	0.385232	3.66
1984	0.09	3.78	2.2	5.50002	0.495001	0.495523	4.88
1985	0.11	4.86	2.3	5.50003	0.605003	0.605848	6.1
1986	0.13	5.4	2.31	5.50003	0.715004	0.716021	7.32
1987	0.15	5.94	2.4	5.50004	0.825005	0.826181	8.54
1988	0.18	6.48	2.42	5.50004	0.990007	0.991348	9.76
1989	0.19	6.75	2.5	5.50004	1.04501	1.04642	11
1990	0.22	7.02	2.53	5.50005	1.21001	1.21150	12.2
1991	0.26	7.56	2.56	5.50005	1.43001	1.43167	13.4
1992	0.32	8.1	2.6	5.50006	1.76002	1.76184	14.6
1993	0.34	9.18	2.62	5.50007	1.87002	1.87219	15.9
1994	0.36	10.3	2.71	5.50008	1.98003	1.98253	17.1
1995	0.37	11.3	2.74	5.50009	2.03503	2.03789	18.3
1996	0.39	11.9	2.78	5.50009	2.14504	2.14806	19.5
1997	0.41	12.4	2.8	5.5001	2.25504	2.25821	20.7
1998	0.42	13	2.9	5.5001	2.31004	2.31355	22
1999	0.43	13.5	3	5.50011	2.36505	2.36852	23.2
2000	0.45	14.6	3.1	5.50012	2.47505	2.47888	24.4
2001	0.46	16.7	3.12	5.50014	2.53060	2.53457	25.6
2002	0.47	18.9	3.2	5.50016	2.58507	2.59026	26.8
2003	0.5	20	3.3	5.50017	2.75008	2.75338	28.1
2004	0.54	20.5	3.4	5.50017	2.97009	2.97576	29.3
2005	0.58	21.6	3.43	5.50018	3.19011	3.19612	30.5
2006	0.59	22.2	3.5	5.50019	3.24511	3.25128	31.7
2007	0.6	22.7	3.55	5.50019	3.30022	3.30644	32.9
2008	0.61	23.2	3.6	5.50020	3.35512	3.36160	34.2

2009	0.62	23.8	3.7	5.50020	3.41012	3.41674	35.4
2010	0.63	24.3	3.8	5.50021	3.46513	3.47190	36.6
2011	0.65	25.4	3.81	5.50022	3.57514	3.58225	37.8
2012	0.68	29.7	3.9	5.50026	3.74018	3.74871	39
2013	0.7	32.4	3.94	5.50029	3.85020	3.85962	40.3
2014	0.74	34	3.97	5.50030	4.07022	4.08017	41.5
2015	0.78	34.6	3.98	5.50031	4.29024	4.30036	42.7
2016	0.8	36.7	4	5.50033	4.40026	4.41108	43.9
2017	0.81	38.9	4.1	5.50035	4.45528	4.4660	45.1
2018	0.82	40	4.11	5.50036	4.51029	4.5220	46.4
2019	0.83	40.5	4.2	5.50036	4.56530	4.5700	47.6
2020	0.85	41.6	4.22	5.50037	4.67532	4.6870	48.8

The specific heat capacity c can be determined graphically from $\Delta Q = f(Z)$, where it corresponds to the slope of the linear dependence in Fig. 1. The value of Z is calculated from experimentally measured atmospheric temperature variations ΔTr. The value of c is obtained from the slope of the first linear segment of the graph in Fig. 1.

$$c = tg\alpha = \frac{\Delta(\Delta Q)}{\Delta Z} = \frac{1{,}01\cdot 10^{21}}{1\cdot 10^{18}} \approx 1010\left(\frac{J}{kg.K}\right) \qquad (23)$$

The dependence of ΔQ shows a smaller slope in the second linear segment as temperature and Z increase. This behavior suggests that the effective specific heat capacity decreases with higher concentrations of atmospheric pollutants. Since the slope of the linear relation corresponds to the specific heat capacity $c=\Delta Q/(m\cdot\Delta T)$, a smaller slope indicates a lower value of c. Therefore, the second linear segment gives:

$$c = tg\alpha = \frac{\Delta(\Delta Q)}{\Delta Z} = \frac{(4{,}5-1{,}01)\cdot 10^{21}}{(4{,}5-1)\cdot 10^{18}} \approx 997\left(\frac{J}{kg.K}\right) \qquad (24)$$

The analysis shows that accumulated atmospheric heat can be described by a semiempirical relation based on thermodynamic calorimetric principles. The excess heat ΔQ depends linearly on atmospheric temperature variation, where m_{atm} (Table 2) is the atmospheric mass and ΔT_r represents measured temperature changes. This linearity is shown in Fig. 2. The specific heat capacity is determined from the slope of the first linear segment.

$$tg\alpha = \frac{1.05\cdot 10^{21}}{0.19} = 5.52\cdot 10^{21} \qquad (25)$$

$$c = \frac{tg\alpha}{m_{atm}} = \frac{5.52\cdot 10^{21}}{5{,}5\cdot 10^{18}} \approx 1004\left(\frac{J}{kg.K}\right) \qquad (26)$$

The second linear segment of Fig. 2 yields the following relationship:

$$tg\alpha = c\cdot m_{atm} = \frac{(4.68-1.05)\cdot 10^{21}}{(0.855-0.19)} = 5.458\cdot 10^{21}$$

$$(27) \quad c = \frac{5.458\cdot 10^{21}}{5.5\cdot 10^{18}} \approx 992\left(\frac{J}{kg.K}\right)$$

(28)

The corresponding dependence $\Delta Q=f(m_{atm}\cdot\Delta T_r)$ is illustrated in Fig. 3. The specific heat capacity, c, can also be determined from the slope of the linear segments. Two distinct segments are observed in Fig. 3. The first segment yields:

$$c = tg\alpha = \frac{\Delta(\Delta Q)}{\Delta(m_{atm}\cdot\Delta T_r)} = \frac{1{,}01\cdot 10^{21}}{1\cdot 10^{18}} \approx 1010\left(\frac{J}{kg.K}\right) \qquad (29)$$

The second segment yields:

$$c = tg\alpha = \frac{\Delta(\Delta Q)}{\Delta(m_{atm}\cdot\Delta T_r)} = \frac{(4.69-1{,}01)\cdot 10^{21}}{(4.71-1)\cdot 10^{18}} \approx 992\left(\frac{J}{kg.K}\right) \qquad (30)$$

The evaluation of the specific heat capacity of atmospheric air is essential because it strongly affects the thermodynamic state of the atmosphere. Atmospheric temperature depends mainly on air composition and specific heat capacity.

Analysis of O_2 and CO_2 trends shows that CO_2 accumulation increases atmospheric mass [30], [31]. Higher greenhouse gas levels reduce specific heat capacity, while greater mass raises density and pressure [54], [55]. Since higher density is linked to lower heat capacity [56], the relation $\Delta Q = f(m_{atm}\cdot\Delta C)$ (Fig. 4) allows estimation of γ, which decreases as pollutants increase.

$$tg\alpha = \frac{(\gamma-1)\cdot c\cdot T}{C} = \frac{(24.1-0)\cdot 10^{20}}{(34-0)\cdot 10^{14}} = 0.7088\cdot 10^{6} \qquad (31)$$

The overall average molar concentration of the atmosphere is C=0.04137 *mol/l.* Using this value, the corresponding parameters in the previously derived expressions can be calculated to quantify the specific heat capacity and the adiabatic constant of atmospheric air under the given conditions.

$$\frac{(\gamma-1)\cdot c\cdot T}{C} = 0.7088\cdot 10^{6};\ (\gamma-1) = \frac{0.7088\cdot 10^{6}\cdot C}{c.T} \qquad (32)$$

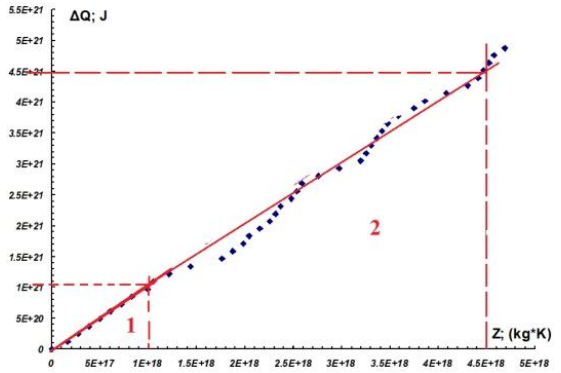

Fig. 1. Calculation of the Specific Heat Capacity of Atmospheric Air Based on Excess Atmospheric Heat (ΔQ).

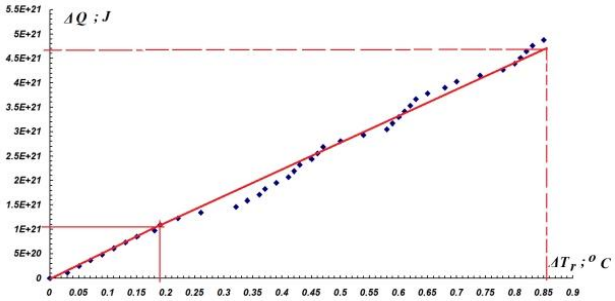

Fig. 2. Atmospheric excess heat variations as a function of temperature change.

For the first segment of Fig. 4, the specific heat capacity of the atmosphere is c=1007 J/(kg·K) and the temperature is T≈288 K. Using these values, the adiabatic constant γ can be calculated as follows:

$$\gamma = 1 + \frac{0.7088 \cdot 10^6 \cdot C}{c.T} = 1.101 \tag{33}$$

The second segment exhibits the following slope:

$$tg\alpha = \frac{(\gamma - 1) \cdot c \cdot T}{C} = \frac{(50.4 - 24.1) \cdot 10^{20}}{(96 - 34) \cdot 10^{14}} = 0.42419 \cdot 10^6 \tag{34}$$

For the second segment of Fig. 4, the specific heat capacity of the atmosphere is c = 992 J/(kg·K) and the temperature is approximately T ≈ 288 K. Using these values, the corresponding adiabatic constant γ can be calculated as follows:

$$\gamma = 1 + \frac{0.42419 \cdot 10^6 \cdot C}{c.T} = 1 + \frac{0.42419 \cdot 10^6 \cdot 0.04137}{992 \cdot 288} = 1.061 \tag{35}$$

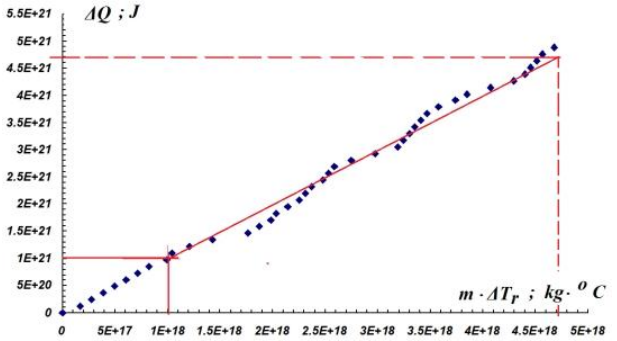

Fig. 3. Changes in atmospheric excess heat as a function of $m_{atm} \cdot \Delta T_r$.

Increasing atmospheric pollution decreases the adiabatic constant γ [57]. In clean air dominated by N_2 and O_2, γ is about 1.4 [50], while lower values (1.101–1.061) indicate higher levels of polyatomic gases and pollutants [58]. These molecules increase heat capacity and reduce γ [59]. The decrease in specific heat to about 992 $J \cdot kg^{-1} \cdot K^{-1}$ affects adiabatic processes, vertical motion, and cloud formation [60]. Since $\gamma = 1 + 2/f$, the low value $\gamma \approx 1.106$ reflects molecular complexity, aerosols, and humidity [10], [13], [57], [58], [60], [61], [62], [63].

Fig. 4 shows that for higher pollutant levels γ is reduced, weaken adiabatic cooling during ascent, and increase buoyancy, instability, storm intensity, and cloud formation. Values are summarized in Table 4 [10], [57], [58], [60], [61], [62].

Atmospheric stability and wind dynamics depend on the thermodynamic properties of air parcels [64]. Pressure gradients drive wind, while polyatomic pollutants lower γ and increase instability [58]. Reduced γ (1.101 → 1.061) causes greater energy storage in molecular modes [10], stronger turbulence and lower predictability [65], slower cooling with $c_p \approx 992$ $J \cdot kg^{-1} \cdot K^{-1}$, and enhanced vertical wind shear and updrafts [65]. These effects are summarized in Table 5 [10], [57], [58], [60], [61], [62].

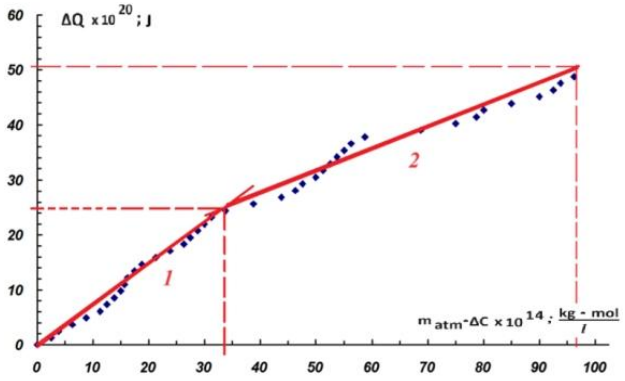

Fig. 4. Graphical dependence of $\Delta Q = f(m_{atm} \cdot \Delta C)$.

TABLE 3 VALUES OF ADIABATIC CONSTANT AS THE FUNCTION OF QUANTITY OF MODES *F* [10], [62], [63]

Category	Pollutant	γ	f	Conc. (mol/L)	Conc. (g/l)
Clean Air	Nitrogen / Oxygen N_2/O_2	1.40	5	4.1×10^{-2}	1.2
Greenhouse Gases	Carbon Dioxide CO_2	1.30	7	1.7×10^{-5}	7.5×10^{-4}
	Methane CH_4	1.32	6	8.2×10^{-8}	1.3×10^{-6}
	Nitrous Oxide N_2O	1.31	7	1.4×10^{-8}	6.2×10^{-7}
	Ozone O_3	1.29	7	2.0×10^{-9}	9.6×10^{-8}
	Sulfur Hexafluoride SF_6	1.09	22	4.0×10^{-13}	5.8×10^{-11}
Acid Rain/Industrial	Sulfur Dioxide SO_2	1.29	6	4.0×10^{-10}	2.6×10^{-8}
	Nitrogen Dioxide NO_2	1.33	6	8.0×10^{-10}	3.7×10^{-8}
VOCs (Aromatics)	Toluene C_7H_8	1.07	28	1.1×10^{-9}	1.0×10^{-7}
	Benzene C_6H_6	1.10	20	6.4×10^{-10}	5.0×10^{-8}
Particulates	$PM_{2.5}$ Aerosol	1.06	33	—	1.5×10^{-7}
	PM_{10} Aerosol	1.04	50	—	4.5×10^{-7}

TABLE 4 THERMODYNAMIC VARIATIONS IN ATMOSPHERIC DEGREES OF FREEDOM AND SPECIFIC HEAT AS A FUNCTION OF POLLUTANT CONCENTRATION [10], [57], [58], [60], [61], [62]

Feature	Segment 1 (Less Polluted)	Segment 2 (More Polluted)
Adiabatic Constant γ	1.101	1.061
Specific Heat (c)	1007 J/(kg K)	992 J/(kg K)
Degrees of Freedom (*f*)	≈ 20	≈ 33
Cooling Profile	Rapid cooling as it rises.	Slower cooling; retains heat longer.

TABLE 5 THERMODYNAMIC MODULATION OF WIND DYNAMICS AND ATMOSPHERIC STABILITY [10], [57], [58], [60], [61], [62]

Metric	High γ (Segment 1)	Low γ (Segment 2 – more Polluted)
Adiabatic Constant	1.101	1.061
Air Response	Sharp pressure changes.	High energy absorption/damping.
Horizontal Wind	Faster propagation of pressure waves.	Potentially more stagnant or turbulent.
Vertical Wind	Standard cooling; stable.	Slower cooling; high buoyancy/instability.

The last part of (20), involving ΔT, Δγ, and Δc_p, shows that increasing temperature ($\Delta T > 0$) generally reduces specific heat capacity ($\Delta c_p < 0$) [66]. The adiabatic constant $\gamma = c_p/c_v$ controls adiabatic processes and supports wind formation through buoyancy [67], [68]. A reduction in γ due to $PM_{2.5}$/PM10 lowers atmospheric stability and suppresses wind development [69]. When γ decreases while T and c_p remain constant, wind speed slightly decreases. The effects are summarized in Table 6 [70], [71].

TABLE 6 EFFECT OF THERMODYNAMIC PARAMETERS ON WIND SPEED [70], [71]

Temp-re; (T)	Specific heat capacity; (C_p)	Adiabatical constant - γ	Wind speed effect
increasing	decreasing	constant	Faster increase
increasing	decreasing	decreasing	Slower increase
constant	constant	decreasing	Slight decrease / lower acceleration

Fig. 5 shows thermodynamic damping of wind velocity due to polyatomic pollutants. The red curve (γ = const) represents the standard adiabatic case, where rising temperature enhances wind acceleration (Δu/u) through buoyancy and the dry adiabatic lapse rate [65], [72]. The blue curve (γ decreasing) represents a polluted atmosphere with aerosols ($PM_{2.5}$, PM_{10}), where increased molecular degrees of freedom reduce γ and suppress wind acceleration by lowering instability [58], [60].

The calculation of first term of (20) yields:

$$\frac{c_p.T}{\sqrt{R}}\cdot\sqrt{\frac{\gamma}{(\gamma-1)\cdot c_p}}=\frac{1007\cdot 288}{\sqrt{8.31}}\cdot\sqrt{\frac{1.4}{0.4\cdot 1007}}=5.8\cdot 10^3 \quad (36)$$

The following cases are examined:

1) $\Delta T \neq 0$; $\Delta c_p \neq 0$; $\Delta\gamma \neq 0$

The variations of temperature **$\Delta T \approx 1$(K); $\Delta c_p \approx -10$ (J/(kg.K)); $\Delta\gamma \approx -0.04$**

$$\left(\frac{1}{2.T}\cdot\frac{\Delta\gamma}{\gamma^2}-\left(\frac{\gamma-1}{\gamma}\right)\frac{\Delta T}{T^2}-\frac{\gamma-1}{2\cdot\gamma\cdot T}\cdot\frac{\Delta c_p}{c_p}\right)=$$

$$=\frac{1}{2\cdot 288}\cdot\left(\frac{-0.04}{1.4^2}\right)-\frac{0.4}{1.4}\cdot\frac{1}{288^2}-\frac{0.4}{2\cdot 1.4\cdot 288}\cdot\left(\frac{-10}{1007}\right)=-33.95\cdot 10^{-6}$$

(37)

$$\frac{\Delta u}{u}=5.8\cdot 10^3\cdot(-33.95)\cdot 10^{-6}=-0.1961 \quad (38)$$

Sometimes the speed of wind is intensified and sometimes is damped drastically. For this case, there is a case of damping of the speed of wind **(≈ - 20%)**.

2) $\Delta T \neq 0$; $\Delta c_p \neq 0$; $\Delta\gamma = 0$

The variations of temperature **$\Delta T \approx 1$(K); $\Delta c_p \approx -10$ (J/(kg.K)); $\Delta\gamma = 0$**

The case when the adiabatical constant is non-changeable (**γ=const**), then **$\Delta\gamma$=0** and the calculations give

$$\left(\frac{1}{2.T}\cdot\frac{\Delta\gamma}{\gamma^2}-\left(\frac{\gamma-1}{\gamma}\right)\frac{\Delta T}{T^2}-\frac{\gamma-1}{2\cdot\gamma\cdot T}\cdot\frac{\Delta c_p}{c_p}\right)=$$

$$=0-\frac{0.4}{1.4}\cdot\frac{1}{288^2}-\frac{0.4}{2\cdot 1.4\cdot 288}\cdot\left(\frac{-10}{1007}\right)=1.48\cdot 10^{-6} \quad (39)$$

$$\frac{\Delta u}{u}=5.8\cdot 10^3\cdot 1.48\cdot 10^{-6}=0.0086 \quad (40)$$

For this case the speed of wind is intensified (is increased) by ≈ 0.86%

3) $\Delta T = 0$; $\Delta c_p = 0$; $\Delta\gamma \neq 0$

The variations of temperature **$\Delta T = 0$; $\Delta c_p = 0$; $\Delta\gamma \approx -0.04$**

$$\left(\frac{1}{2.T}\cdot\frac{\Delta\gamma}{\gamma^2}-\left(\frac{\gamma-1}{\gamma}\right)\frac{\Delta T}{T^2}-\frac{\gamma-1}{2\cdot\gamma\cdot T}\cdot\frac{\Delta c_p}{c_p}\right)=$$

$$=\frac{1}{2\cdot 288}\cdot\left(\frac{-0.04}{1.4^2}\right)-0-0=-3.543\cdot 10^{-5} \quad (41)$$

$$\frac{\Delta u}{u}=5.8\cdot 10^3\cdot(-35.43)\cdot 10^{-6}=-0.205 \quad (42)$$

Wind speed decreases by about 21%. Pollutants reduce wind through thermodynamic damping and aerosol–meteorology feedback [73], [74], [75], [76]. PM2.5, PM10, and black carbon act through radiative forcing, atmospheric stabilization, and thermodynamic damping, where higher molecular complexity raises c_p and lowers γ, reducing wind speed [77], [78], [73], [75], [79], [80], [81], [82], [76], [83], [84]. Studies show strong negative correlations ($r \approx -0.8$) between pollution and wind speed [81], [82], with long-term aerosol-driven terrestrial stilling [73], [78].

Since the values of albedo increase with time ($\Delta A > 0$) [48], the change in wind speed obtained from (27) may become positive, which indicates an increase in wind speed ($\Delta u > 0$). The contributions to the change of speed are presented in Table 7.

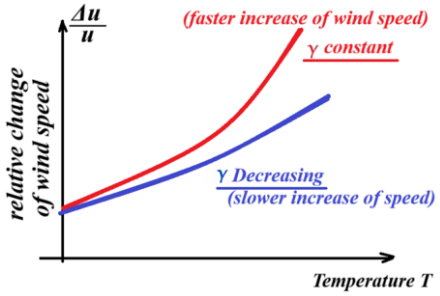

Fig. 5. Thermodynamic Damping of Wind Velocity by Polyatomic Pollutants.[43-45]

TABLE 7 INFLUENCE OF THERMODYNAMIC AND ALBEDO FEEDBACK TERMS ON WIND VELOCITY

Contribution	Sign	Effect on Wind
Direct thermodynamic terms ($\Delta\gamma$, Δc_p)	Negative	Decrease wind
Albedo feedback term (ΔA)	Positive	Increase wind

In general (22) contains four important terms

1) Term: $\frac{\Delta\gamma}{2\cdot\gamma^2}$. The adiabatic constant decreases over time due to the presence of larger pollutant molecules in the atmosphere. This effect tends to reduce wind speeds.
2) Term: $-\frac{(\gamma-1)\cdot T\cdot\Delta c_p}{\gamma\cdot 2\cdot c_p}$. This term is associated with changes in the specific heat capacity. A decrease in the specific heat capacity over time leads to a positive contribution of this term, which, together with the first term, results in a slower decrease in wind speed. If the second term is absent, the first term alone would lead to a faster decrease in wind speed.
3) Term: $-\frac{(\gamma-1)}{\gamma\cdot T}\cdot\left(\frac{\Delta Q}{m.c}-\frac{Q\cdot\Delta m}{m^2.c}\right)$. This term represents the thermal driving caused by excess heat and mass variations. Its value may be positive or negative depending on the magnitudes of ΔQ and Δm.
4) Term: $\frac{(\gamma-1)\cdot\Delta A}{\gamma\cdot T\cdot K}$. Wind speed variation depends on the balance between thermodynamic changes ($\Delta\gamma$, Δc_p), thermal forcing (ΔQ, Δm), and radiative effects (ΔA). Increased albedo from sulfate aerosols can enhance wind speed, while the first three terms cause thermodynamic damping. Wind increases or decreases depending on which effect dominates. Atmospheric regimes are summarized in Table 8.

To determine whether winds are damping or accelerating, a special ratio, called the feedback ratio (Φ), is defined.

$$\Phi = \frac{Albedo\ term}{Therm-ic\quad terms} = \frac{\frac{\gamma-1}{\gamma.T}\cdot\frac{\Delta A}{K}}{\left[\frac{\Delta\gamma}{2\cdot\gamma^2}-\frac{(\gamma-1)\cdot T\cdot\Delta c_p}{\gamma\cdot 2\cdot c_p}-\frac{(\gamma-1)}{\gamma\cdot T}\cdot\left(\frac{\Delta Q}{m.c}-\frac{Q\cdot\Delta m}{m^2.c}\right)\right]} \quad (43)$$

If Φ<1, then wind decreases (polluted dominated regime).
If Φ>1, then wind increases (albedo dominated regime).
If Φ≈1, then we have bistability or tipping points.

TABLE 8 IMPACT OF DIFFERENT ATMOSPHERIC REGIMES ON WIND VIA ALBEDO AND THERMODYNAMIC EFFECTS

Regime	Dominant Term	Net Effect on Wind
Clean atmosphere	Albedo term small	Slight decrease or stable
Marine aerosols	Albedo term moderate	Near-zero (stabilizing feedback)
Black carbon / $PM_{2.5}$	Thermodynamic terms dominate	Strong decrease (damping)
Hypothetical pure-albedo	Albedo term dominates	Wind increase (rare)

The regime of Pollution dominated or albedo dominated is presented in Table 9.

TABLE 9 SUMMARY OF POLLUTANT TYPES AND THEIR CORRESPONDING THERMODYNAMIC CHARACTERISTICS

Pollutant	γ	Type	Regime
Clean Air (N_2/O_2)	1.40	Background	Clean
CO_2	1.30	GHG	Pollution-Dominated (if dominant)
CH_4	1.32	GHG	Pollution-Dominated
SO_2	1.29	Scattering aerosol	Albedo-Dominated (if dominant)
Black Carbon	~1.06 (with PM)	Absorbing aerosol	Pollution-Dominated
$PM_{2.5}$	~1.06	Complex mix	Pollution-Dominated
Sea Salt	~1.33 (estimate)	Scattering	Albedo-Dominated

Then, (22) shows that wind speed is determined by a balance:

$$\frac{\Delta u}{u} = Negative\ Therm-ic\ Terms\ +\ Positive\ \ Albedo\ Term$$

Whether wind increases or decreases depends on which term dominates. The net effect on wind is presented in Table 10.

This relation shows two competing responses to pollution: thermodynamic damping, which reduces wind speed, and albedo forcing, which can enhance wind activity. The net effect depends on aerosol composition: clean or marine aerosols keep stable conditions, black carbon and soot cause wind stilling, while volcanic or marine events may temporarily increase wind. Table 11 summarizes these effects through the feedback ratio Φ.

TABLE 10 SUMMARY OF ATMOSPHERIC REGIMES AND THEIR IMPACT ON WIND DYNAMICS

Regime	Dominant Term	Net Effect on Wind
Clean atmosphere	Albedo term small	Slight decrease or stable
Marine aerosols	Albedo term moderate	Near-zero (stabilizing feedback)
Black carbon/ $PM_{2.5}$	Thermodynamic terms dominate	Strong decrease (damping)
Hypothetical pure-albedo	Albedo term dominates	Wind increase (rare)

1) Albedo dominated regime Φ>1. This regime is described by more aerosols. For the albedo dominated regime is characteristic that this regime occurs when

$$\frac{(\gamma-1)}{\gamma.T}\cdot\frac{\Delta A}{K} > |Therm-ic\quad Terms| \quad (44)$$

Physical characteristics:
• Aerosols: mainly scattering (sulfates SO_4^{2-}, sea salt, ammonium nitrate)
• Cloud effect: increased Cloud Condensation Nuclei (CCN) → smaller droplets → brighter clouds (Twomey effect)
• GHG levels: low–moderate (CO_2, CH_4 not dominant)
• Molecular effect: small Δγ and Δcp (minor change in composition)
• Result: wind slightly increases or remains stable.

2) Pollution dominated regime (Φ<1). This regime is described by more green house gases and absorbing aerosols. This regime occurs when:

$$\frac{(\gamma-1)}{\gamma.T}\cdot\frac{\Delta A}{K} < |Therm-ic\quad Terms| \quad (45)$$

Physical characteristics:
• Aerosol type: absorbing aerosols (black carbon, brown carbon, dust) + polyatomic gases (CO_2, CH_4, N_2O)
• Molecular effect: significant changes in Δγ and Δcp, altering air composition
Typical γ values:
Clean air: γ ≈ 1.40
CO_2: γ ≈ 1.30
CH_4: γ ≈ 1.32
$PM_{2.5}$: γ ≈ 1.06
Result: wind decreases due to thermodynamic damping.

TABLE 11 CLASSIFICATION OF ATMOSPHERIC FORCING REGIMES BASED ON AEROSOL AND GREENHOUSE GAS LOADING

Regime	Physical Meaning	Primary Driver	Aerosol Load	GHG Load
Albedo-Dominated (Φ>1)	Reflection effects dominate over thermodynamic effects	Scattering aerosols (sulfates, sea salt, clean clouds)	High	Low to Moderate
Pollution-Dominated (Φ<1)	Thermodynamic/ molecular effects dominate	Absorbing aerosols + GHGs (black carbon, $PM_{2.5}$, CO_2, CH_4)	High	High
Clean Regime (Φ≈1)	No significant forcing	Natural background	Low	Low

Table 12 presents four atmospheric regimes defined by GHG and aerosol levels, showing their effects on radiative forcing (Φ) and wind patterns. GHGs enhance warming and circulation changes, while aerosols modify albedo and often reduce surface wind speed ("wind stilling").

TABLE 12 CLIMATE INTERACTION MATRIX: GREENHOUSE GASES VS. AEROSOLS

	Low Aerosols	High Aerosols
Low GHGs	Clean Regime (Φ≈1) • Natural winds • Small Δu	Albedo-Dominated (Φ>1) • Marine/volcanic • Wind stable or ↑
High GHGs	GHG-Only Warming • ΔT ↑ • Complex wind	Pollution-Dominated (Φ<1) • BC + CO_2 + CH_4 • Wind stilling (Δu/u < 0)

CONCLUSIONS

This research established a combined model that connects thermodynamic properties of air with radiative feedback processes in order to explain how atmospheric pollution changes wind speed. The results show that pollution influences not only the chemical state of the atmosphere but also the basic physical principles that control air movement, convection, and energy transfer.

One of the central findings concerns the thermodynamic modification of polluted air. In cleaner atmospheric conditions, the specific heat capacity of air is close to 1007 J/kg·K, while in strongly polluted environments it decreases to nearly 992 J/kg·K. At the same time, the adiabatic constant gamma decreases from 1.101 to 1.061. This variation corresponds to an increase in the effective molecular degrees of freedom from about 20 to nearly 33, indicating that pollution changes the way energy is distributed within atmospheric molecules.

These changes have a strong effect on the vertical thermal profile of the atmosphere. A lower value of the adiabatic constant causes weaker adiabatic cooling when air rises upward. As a result, atmospheric instability becomes stronger, convection is modified, and vertical wind transport changes noticeably. This confirms that pollution directly affects the thermodynamic balance responsible for atmospheric circulation.

Another major result is the definition of different wind response regimes controlled by the feedback parameter Φ.

This ratio determines whether pollution produces weaker winds or supports stronger circulation. When $\Phi < 1$, the pollution-dominated regime is established. In this situation, thermodynamic damping becomes dominant and wind speed may decrease by up to 20 percent. This behavior is typical for black carbon, PM2.5 aerosols, and high greenhouse gas concentrations. When $\Phi > 1$, the atmosphere enters the albedo-dominated regime. Scattering aerosols such as sulfates and sea salt increase atmospheric reflectivity, which improves stability and can preserve or slightly increase wind speed. When $\Phi \approx 1$, the system reaches a critical transition region with bistable behavior. In this zone, small changes in aerosol composition may shift the atmosphere from one regime to another, creating tipping-point effects in wind dynamics.

An additional important result is the derived mathematical relation between relative wind speed variation ($\Delta u/u$) and changes in temperature (ΔT), specific heat capacity (Δc_p), adiabatic constant ($\Delta\gamma$), and albedo (ΔA). This equation shows the balance between thermodynamic suppression and radiative compensation. An increase in albedo ($\Delta A > 0$) can partly compensate for wind reduction by reflecting more incoming solar radiation. However, strongly absorbing aerosols such as black carbon dominate over this effect, leading to net wind stilling.

The practical applications of this work are broad. In climate modeling, it becomes necessary to include aerosol composition, especially the difference between scattering and absorbing particles, together with greenhouse gases for accurate prediction of atmospheric circulation. In air quality management, reducing black carbon and PM2.5 emissions can help prevent wind stilling and improve pollutant dispersion. For renewable energy planning, wind resource assessment should consider regional aerosol conditions, such as differences between marine and industrial zones. In urban planning, cities with high concentrations of absorbing aerosols may experience weaker ventilation, which can intensify heat island effects and increase pollution episodes.

The broader significance of the study is that pollution changes not only radiative forcing but also the fundamental thermodynamic properties of air itself. Ignoring these coupled effects may lead to serious errors in predicting wind patterns, storm behavior, and boundary-layer processes. Future climate studies should therefore include composition - dependent parameres of specific hea capcity and the adiabatic constant in order to describe the full anthropogenic impact on atmospheric circulation more accurately.

REFERENCES

[1] Petrov, M., 2021. Adiabatical thermodynamic manner of the description of the carbon dioxide pollutant excess of Earth's atmosphere. In: *Proceedings of the V International Scientific Conference on Mathematical Modelling*, Borovets, Bulgaria, 8–11 December 2021. *Mathematical Modelling*, 5(3), 8–15.

[2] U.S. Standard Atmosphere, 1976. Engineering ToolBox. Available at: https://www.engineeringtoolbox.com/standard-atmosphere-d_604.html

[3] NASA Earth Observatory, 2023. World of Change: Global Temperatures. https://earthobservatory.nasa.gov/world-of-change/global-temperatures

[4] Copernicus Climate Change Service, 2019. Last four years have been the warmest on record and CO_2 continues to rise. https://climate.copernicus.eu

[5] Electrical and Mechanical Services Department (EMSD), 2023. *Energyland: Greenhouse Gases*. Government of the Hong Kong Special Administrative Region. Available at: https://www.emsd.gov.hk/energyland

[6] Petrov, M., 2021. Major contribution of carbon dioxide excess in atmosphere to the greenhouse effect. *Oxidation Communications*, 44(4), 870–907.

[7] Antweiler, W., 2015. *Fossil fuels and declining oxygen in our atmosphere*. Available at: https://wernerantweiler.ca/blog.php?item=2015-10-15

[8] Vashishta, M., Sharma, P., 2014. Variation of specific heat ratio. *International Journal of Engineering and Advanced Technology*, 3(4), 213–217.

[9] Seinfeld, J.H., Pandis, S.N., 2016. *Atmospheric Chemistry and Physics: From Air Pollution to Climate Change*, 3rd ed. Wiley, Hoboken, NJ.

[10] Manatung, S.S., Latimer, D.C., 2019. Heat capacity ratios of real gases. *Journal of Chemical Education*, 96, 1694–1700. https://doi.org/10.1021/acs.jchemed.9b00060

[11] Wejlah, A.K., 2025. Thermophysical properties of atmospheric gases. *South Eastern European Journal of Public Health*, 26(S2), pp. 3809–3817. https://doi.org/10.70135/seejph.vi.5859

[12] Petrov, M., et al., 2025. Influence of greenhouse pollutants on adiabatic constant. In: *Modelling and Development of Intelligent Systems*. Springer.

[13] White, F.M., 2011. *Fluid Mechanics*, 7th ed. McGraw-Hill.

[14] Chen, R.H., 2017. *Foundations of Gas Dynamics*. Cambridge University Press.

[15] Twomey, S., 1977. The influence of pollution on the shortwave albedo of clouds. *Journal of the Atmospheric Sciences*, 34, 1149–1152. https://doi.org/10.1175/1520-0469(1977)034<1149:TIOPOT>2.0.CO;2

[16] Lohmann, U., Feichter, J., 2005. Global indirect aerosol effects: a review. *Atmospheric Chemistry and Physics*, 5, 715–737. https://doi.org/10.5194/acp-5-715-2005

[17] Ritchie, H., Roser, M., 2021. *Deforestation and Forest Loss*. Our World in Data. Available at: https://ourworldindata.org/deforestation

[18] Hansen, J., Nazarenko, L., 2004. Soot climate forcing via snow and ice albedos. *PNAS*, 101(2), 423–428. https://doi.org/10.1073/pnas.2237157100

[19] Menon, S., et al., 2010. Radiative forcing and temperature response to changes in urban albedos. *Environmental Research Letters*, 5(1). https://doi.org/10.1088/1748-9326/5/1/014005

[20] Cugliandolo, L.F., 2011. Effective temperature of the Earth. *Journal of Physics A*, 44, 483001. https://doi.org/10.1088/1751-8113/44/48/483001

[21] Latham, J., Smith, M.H., 1990. Effect on global warming of wind-dependent aerosol generation. *Nature*, 347, 372–373. https://doi.org/10.1038/347372a0

[22] Ramanathan, V., Carmichael, G., 2008. Global and regional climate changes due to black carbon. *Nature Geoscience*, 1, 221–227. https://doi.org/10.1038/ngeo156

[23] Lide, D.R. (Ed.), 1996. *CRC Handbook of Chemistry and Physics*, 77th ed. CRC Press, Boca Raton.

[24] Kelly, M., Monroe, R., 2018. *Earth's oceans have absorbed 60 percent more heat per year than previously thought*. Princeton University. Available at: https://www.princeton.edu/news/2018/10/31

[25] Berlinger, J., Smith-Spark, L., 2018. *World's oceans have absorbed 60 percent more heat than previously thought*. CNN. Available at: https://edition.cnn.com/2018/10/31/world/ocean-warming-study

[26] McCarthy, J., 2018. *Oceans have absorbed 60 percent more heat than previously thought*. Global Citizen. Available at: https://www.globalcitizen.org

[27] Shutler, J., Watson, A., 2020. *The oceans are absorbing more carbon than previously thought*. Carbon Brief. Available at: https://www.carbonbrief.org

[28] Oceanographic Magazine, 2021. *Rate of CO_2 absorption by ocean impacted by human-caused atmospheric changes*. Available at: https://www.oceanographicmagazine.com

[29] Picone, J.M., Hedin, A.E., Drob, D.P., Aikin, A.C., 2002. NRLMSISE-00 empirical model of the atmosphere. *Journal of Geophysical Research: Space Physics*, 107(A12), 1468. https://doi.org/10.1029/2002JA009430

[30] Chemke, R., Kaspi, Y., Halevy, I., 2016. The thermodynamic effect of atmospheric mass on early Earth's temperature. *Geophysical Research Letters*, 43, 11414–11422. https://doi.org/10.1002/2016GL071279

[31] Best, C., 2016. *The atmosphere is getting heavier*. Available at: https://clivebest.com/blog/?p=7704

[32] Raju, D., Ramdin, M., Vlugt, T.J.H., 2024. Thermophysical properties of CO_2 with impurities. *Journal of Chemical & Engineering Data*, 69(8), 2735–2755. https://doi.org/10.1021/acs.jced.4c00164

[33] Ning, F.L., et al., 2015. Heat capacity of CH_4–CO_2 mixtures. *Physical Chemistry Chemical Physics*, 17, 2869–2883. https://doi.org/10.1039/C4CP04725A

[34] Colman, R., 2021. Water vapor and lapse rate feedbacks. *Reviews of Modern Physics*, 93, 045002. https://doi.org/10.1103/RevModPhys.93.045002

[35] Manabe, S., 2019. Role of greenhouse gases in climate change. *Climate Dynamics*, 53, 113–129. https://doi.org/10.1007/s00382-018-4137-6

[36] Henry, M., Merlis, T.M., 2020. Forcing dependence of atmospheric lapse rate changes. *Geophysical Research Letters*, 47, e2020GL087929. https://doi.org/10.1029/2020GL087929

[37] Brogli, R., et al., 2021. Lapse rate effects on future summer warming. *Weather and Climate Dynamics*, 2, 1093–1110. https://doi.org/10.5194/wcd-2-1093-2021

[38] Wong, G.S.K., Embleton, T.F.W., 1984. Variation of specific heats in humid air. *Journal of the Acoustical Society of America*, 76, 555–559. https://doi.org/10.1121/1.391002

[39] Liepmann, H.W., Roshko, A., 2001. *Elements of Gasdynamics*. Dover.

[40] Liou, K.N., 2002. *An Introduction to Atmospheric Radiation*, 2nd ed. Academic Press. https://doi.org/10.1016/B978-012451451-5/50001-8

[41] Ramanathan, V., Crutzen, P.J., Kiehl, J.T., Rosenfeld, D., 2001. Aerosols, climate, and the hydrological cycle. *Science*, 294(5549), 2119–2124. https://doi.org/10.1126/science.1064034

[42] Merenda, B., et al., 2024. PM variability and meteorology. *Scientific Reports*, 14, 19461. https://doi.org/10.1038/s41598-024-19461

[43] Twomey, S., 1974. Pollution and the planetary albedo. *Atmospheric Environment*, 8, 1251–1256. https://doi.org/10.1016/0004-6981(74)90004-3

[44] Andreae, M.O., Rosenfeld, D., 2008. Aerosol–cloud–precipitation interactions. *Earth-Science Reviews*, 89, 13–41. https://doi.org/10.1016/j.earscirev.2008.03.001

[45] Bond, T.C., et al., 2013. Bounding the role of black carbon in the climate system. *Journal of Geophysical Research*, 118, 5380–5552. https://doi.org/10.1002/jgrd.50171

[46] Wild, M., 2009. Global dimming and brightening. *Journal of Geophysical Research*, 114. https://doi.org/10.1029/2008JD011470

[47] Oke, T.R., 1987. *Boundary Layer Climates*, 2nd ed. Routledge.
[48] Petrov, M., 2022. Relational empirical study of outgoing longwave radiation–albedo–temperature of the atmosphere–Earth system under the influence of carbon dioxide pollutants. *Oxidation Communications*, 45(2), 350–382.
[49] IPCC, 2021. *Climate Change 2021: The Physical Science Basis*. Cambridge University Press. https://www.ipcc.ch/report/ar6/wg1
[50] Wallace, J.M., Hobbs, P.V., 2006. *Atmospheric Science: An Introductory Survey*, 2nd ed. Academic Press.
[51] Holton, J.R., Hakim, G.J., 2013. *An Introduction to Dynamic Meteorology*, 5th ed. Academic Press.
[52] Landau, L.D., Lifshitz, E.M., 1980. *Statistical Physics. Part 1*, 3rd ed. Pergamon Press, Oxford. https://doi.org/10.1016/C2009-0-07734-5
[53] Lemmon, E.W., Jacobsen, R.T., Penoncello, S.G., Friend, D.G., 2000. Thermodynamic properties of air and mixtures of nitrogen, argon, and oxygen from 60 to 2000 K. *Journal of Physical and Chemical Reference Data*, 29(3), 331–385. https://doi.org/10.1063/1.1285884
[54] Trenberth, K.E., Smith, L., 2004. The mass of the atmosphere: A constraint on global analyses. *Journal of Climate*, 17, 864–875. https://doi.org/10.1175/1520-0442(2004)017<0864:TMOATA>2.0.CO;2
[55] Ball, P., 2003. Global greenhouse effects air pressure. *Nature*, 422, 245. https://doi.org/10.1038/422245a
[56] Almousa, N., et al., 2021. Paraffin wax composites for thermal energy storage. *Crystals*, 11, 951. https://doi.org/10.3390/cryst11080951
[57] Mayer, H., 2000. Air pollution in cities. *Solar Energy*, 69(6), 427–436. https://doi.org/10.1016/S0038-092X(00)00004-1
[58] Zha, J., et al., 2021. Aerosol forcing and wind stilling. *Environmental Research Letters*, 16, 064002. https://doi.org/10.1088/1748-9326/ac02c8
[59] Mason, E.A., Saxena, S.C., 1958. Transport properties of gases. *Physics of Fluids*, 1(5), 361–369. https://doi.org/10.1063/1.1724352
[60] Pruppacher, H.R., Klett, J.D., 2010. *Microphysics of Clouds and Precipitation*, 2nd ed. Springer.
[61] Berberan-Santos, M.N., et al., 2005. On the barometric formula. *American Journal of Physics*, 73, 914–923. https://doi.org/10.1119/1.1900108
[62] Lemmon, E.W., Jacobsen, R.T., 2004. Transport properties of air. *Journal of Physical and Chemical Reference Data*, 33, 195–235. https://doi.org/10.1063/1.1645272
[63] Myhre, G., et al., 2013. Anthropogenic and natural radiative forcing. In: *Climate Change 2013: The Physical Science Basis*. Cambridge University Press.
[64] Bohren, C.F., Albrecht, B.A., 2000. *Atmospheric Thermodynamics*. Oxford University Press.
[65] Stull, R.B., 1988. *Boundary Layer Meteorology*. Springer.
[66] Petrov, M., et al., 2024. *Thermodynamic empirism for atmospheric pollutants*. *Environment. Technology. Resources*, 1, pp. 300–305.
[67] Fuchs, R., Glasser, L., 2022. Rüchardt experiment. Springer.
[68] Shaw, T.A., 2025. Moist adiabatic scaling. *Geophysical Research Letters*, 52(7).
[69] Yang, Q., et al., 2017. *$PM_{2.5}$ and meteorological factors*. arXiv preprint. Available at: https://arxiv.org
[70] Ames, F.E., Tang, C.C., 2021. *Compressible Flow*. CRC Press.
[71] Kundu, P.K., et al., 2015. *Fluid Mechanics*, 6th ed. Academic Press.
[72] Su, T., et al., 2020. Aerosol-boundary layer feedback. *Journal of Geophysical Research: Atmospheres*, 125. https://doi.org/10.1029/2019JD031975
[73] Zhang, Y., et al., 2020. Dome effect of black carbon. *Atmospheric Research*, 239, 104921. https://doi.org/10.1016/j.atmosres.2019.104921
[74] Naydenova, S., et al., 2022. PAHs in $PM_{2.5}$ and PM_{10}. *Journal of Environmental Science and Health A*, 57, 1–12. https://doi.org/10.1080/10934529.2022.2036789
[75] Nikolaeva, Z., et al., 2017. *Atmospheric transparency and PM_{10}. International Journal of Scientific Engineering and Applied Science*, 3(5), pp. 109–114.
[76] Dimitrov, A., Naydenova, S., 2025. Black carbon in $PM_{2.5}$. *Atmosphere*, 16(2), 412. https://doi.org/10.3390/atmos16020412
[77] Gui, K., et al., 2021. Aerosol–boundary layer feedback. *Environment International*, 157, 106861. https://doi.org/10.1016/j.envint.2021.106861
[78] Ren, Y., et al., 2021. Aerosol-boundary layer feedback. *Atmospheric Chemistry and Physics*, 21, 9033–9047. https://doi.org/10.5194/acp-21-9033-2021
[79] Dimitrov, A., Naydenova, S., 2023. Thermodynamic damping of wind velocity. *Journal of Atmospheric and Solar-Terrestrial Physics*, 248, 106004. https://doi.org/10.1016/j.jastp.2023.106004
[80] Naydenova, S., et al., 2022. *Atmospheric PM levels*. *Journal of Environmental Science and Health, Part A*, 57, pp. 1–12. https://doi.org/10.1080/10934529.2022.2036789
[81] Dimitrov, A., 2021. Adiabatic processes in polluted atmospheres. *Bulgarian Chemical Communications*, 53(A), 112–118.
[82] Dimitrov, A., Naydenova, S., 2025. Black carbon and meteorology. In: *Proceedings of the VII ICABLS*, pp. 1023–1034.
[83] Hartmann, D.L., 2016. *Global Physical Climatology*, 2nd ed. Elsevier. https://doi.org/10.1016/C2012-0-04052-0
[84] Hansen, J., Sato, M., Ruedy, R., 1997. Radiative forcing and climate response. *Journal of Geophysical Research*, 102(D6), 6831–6864. https://doi.org/10.1029/96JD03436